HHS Public Access

Author manuscript

Basic Res Cardiol. Author manuscript; available in PMC 2016 November 15.

Published in final edited form as:

Basic Res Cardiol. 2015 September ; 110(5): 505. doi:10.1007/s00395-015-0505-6.

Expression and function of Kv1.1 potassium channels in human atria from patients with atrial fibrillation

Edward Glasscock[1], **Niels Voigt**[2,3], **Mark D. McCauley**[4], **Qiang Sun**[2,3], **Na Li**[4], **David Y. Chiang**[4], **Xiao-Bo Zhou**[3], **Cristina E. Molina**[2], **Dierk Thomas**[3], **Constanze Schmidt**[3], **Darlene G. Skapura**[4], **Jeffrey L. Noebels**[5,6,7], **Dobromir Dobrev**[2,3], and **Xander H. T. Wehrens**[4]

[1]Department of Cellular Biology and Anatomy, Louisiana State University Health Sciences Center, 1501 Kings Highway, P.O. Box 33932, Shreveport, LA 71130-393, USA

[2]Faculty of Medicine, Institute of Pharmacology, University Duisburg-Essen, Essen, Germany

[3]Division of Experimental Cardiology, Medical Faculty Mannheim, University of Heidelberg, Mannheim, Germany

[4]Department of Molecular Physiology and Biophysics, and Medicine/Cardiology, Cardiovascular Research Institute, Baylor College of Medicine, Houston, TX, USA

[5]Departments of Neurology, Baylor College of Medicine, Houston, TX, USA

[6]Departments of Neuroscience, Baylor College of Medicine, Houston, TX, USA

[7]Departments of Molecular and Human Genetics, Baylor College of Medicine, Houston, TX, USA

Abstract

Voltage-gated Kv1.1 channels encoded by the *Kcna1* gene are traditionally regarded as being neural-specific with no known expression or intrinsic functional role in the heart. However, recent studies in mice reveal low-level Kv1.1 expression in heart and cardiac abnormalities associated with Kv1.1-deficiency suggesting that the channel may have a previously unrecognized cardiac role. Therefore, this study tests the hypothesis that Kv1.1 channels are associated with arrhythmogenesis and contribute to intrinsic cardiac function. In intra-atrial burst pacing experiments, *Kcna1*-null mice exhibited increased susceptibility to atrial fibrillation (AF). The atria of *Kcna1*-null mice showed minimal Kv1 family ion channel remodeling and fibrosis as measured by qRT-PCR and Masson's trichrome histology, respectively. Using RT-PCR, immunocytochemistry, and immunoblotting, *KCNA1* mRNA and protein were detected in isolated mouse cardiomyocytes and human atria for the first time. Patients with chronic AF (cAF) showed no changes in *KCNA1* mRNA levels relative to controls; however, they exhibited increases in atrial Kv1.1 protein levels, not seen in paroxysmal AF patients. Patch-clamp recordings of isolated human atrial myocytes revealed significant dendrotoxin-K (DTX-K)-sensitive outward current components that were significantly increased in cAF patients, reflecting a contribution by Kv1.1

✉Edward Glasscock, aglas1@lsuhsc.edu.

Electronic supplementary material The online version of this article (doi:10.1007/s00395-015-0505-6) contains supplementary material, which is available to authorized users.

Compliance with ethical standards

Conflicts of interest None.

channels. The concomitant increases in Kv1.1 protein and DTX-K-sensitive currents in atria of cAF patients suggest that the channel contributes to the pathological mechanisms of persistent AF. These findings provide evidence of an intrinsic cardiac role of Kv1.1 channels and indicate that they may contribute to atrial repolarization and AF susceptibility.

Keywords

Voltage-gated potassium channels; Atrial fibrillation; Dendrotoxin-K; *Kcna1*; Kv1.1

Introduction

Atrial fibrillation (AF) is the most common sustained cardiac arrhythmia and associated with significant cardiovascular morbidity and mortality, but its underlying molecular basis remains only partially understood [47]. During AF, atrial cells fire rapidly at rates up to tenfold faster than normal, producing uncoordinated atrial activity and irregular ventricular contraction, which can lead to blood clot formation and stroke [21]. Alteration of ion channel function by atrial remodeling or genetic mutation can provide a pro-fibrillatory electrophysiological substrate conducive to AF [13, 22]. A variety of conditions can cause ion channel remodeling predisposing to AF, including congestive heart failure and acute myocardial infarction [23]. In addition, AF itself can cause electrical remodeling that promotes persistent fibrillation and thereby auto-perpetuates the arrhythmia. The underlying mechanisms for this transition likely involve altered channel expression and function [22, 23, 50]. Although AF is primarily a sporadic condition, population-based studies and rare familial kindreds have shown that it has a significant genetic component [19, 35]. In families with monogenic AF subtypes, the majority of genes implicated encode subunits of voltagegated potassium and sodium channels [19].

Here Kv1.1 voltage-gated potassium channels were investigated for a role in AF. Kv1.1 channels, encoded by the *Kcna1* gene, exhibit widespread expression throughout the brain and peripheral nervous system and their dysfunction leads to neurological diseases including epilepsy and episodic ataxia type 1 [29]. Kv1.1 channels have traditionally been regarded as predominantly neural-specific with no known expression or function in the heart. However, mice lacking Kv1.1 channels exhibit atrioventricular cardiac conduction abnormalities and bradyarrhythmia phenotypes that appear to emanate from seizures and abnormal vagal activity [10, 11]. In addition, these previous studies detected low levels of *Kcna1* mRNA and protein in mouse heart suggesting that Kv1.1 channels may also contribute to the intrinsic function of the heart [11]. If so, alteration of Kv1.1 channel function could lead to independent dual arrhythmia phenotypes in brain and heart.

In this work, a combination of electrophysiological techniques and molecular analyses was used to evaluate the contribution of Kv1.1 channels to basal cardiac function and potential arrhythmia development. Two main hypotheses were tested: (1) that Kv1.1 channel perturbation in mice causes arrhythmia susceptibility, and (2) that dysregulation of Kv1.1 channels in the human heart may be important for arrhythmogenesis. Our experiments show that the absence of Kv1.1 channels predisposes the mouse heart to AF without drastic

remodeling of related K+ channel subunits and fibrotic structural changes. Expression analyses in isolated mouse myocytes demonstrate the presence of Kv1.1 mRNA and protein in heart apart from neural tissue. Molecular analyses detect the first clear evidence of Kv1.1 expression in human atria, and show that Kv1.1 channels exhibit expression changes in patients with chronic AF suggestive of pathophysiological channel remodeling. In addition, patch-clamp recordings of isolated human atrial myocytes reveal significant DTX-K-sensitive components that are doubled in patients with cAF, indicative of a contribution by Kv1.1 channels. Taken together this work finds a previously unrecognized cardiac role for the *Kcna1* gene and Kv1.1 channels in regulating atrial repolarization and arrhythmia susceptibility.

Methods

Animals and genotyping

Kcna1$^{-/-}$ mice carry null alleles of the *Kcna1* gene resulting from targeted deletion of the open reading frame, as described [36]. The mice are maintained on a Tac:N:-NIHS-BC background. Animals were housed at 22 °C, fed ad libitum, and submitted to a 12 h light/dark cycle. For surgeries, mice were anaesthetized using 1.5–2 % isoflurane in 95 % O_2. Animals were euthanized for expression and tissue analysis using inhaled isoflurane overdose. All procedures were performed in accordance with the guidelines of the National Institutes of Health, as approved by the Animal Care and Use Committee of Baylor College of Medicine.

Genomic DNA was isolated by enzymatic digestion of tail clips using Direct-PCR Lysis Reagent (Viagen Biotech, Los Angeles, CA, USA). The genotypes of *Kcna1* mice were determined by performing PCR amplification of genomic DNA using three allele-specific primers: a mutant-specific primer (5′-CCTTCTATCGCCTTCTTGACG-3′), a wild-type-specific primer (5′-GCCTCTGACAGTGACCTCAGC-3′), and a common primer (5′-GCTTCAGGTTCGCCACTCCCC-3′). The PCR yielded amplicons of ~337 bp for the wild-type allele and ~475 bp for the null allele.

Intracardiac electrophysiology in mice

In vivo electrophysiology studies were performed in knockout and wild-type mice of both sexes, as per prior established protocols [15, 37]. Atrial and ventricular intracardiac electrograms were recorded simultaneously using a 1.1F octapolar catheter (EPR-800, Millar Instruments, Houston, TX, USA) inserted via the right jugular vein. Surface ECG and intracardiac electrophysiology parameters were assessed at baseline. Right atrial pacing was performed using 2-ms current pulses at 800 μA delivered by an external stimulator (STG-3008, Multi Channel Systems, Reutlingen, Germany). AF inducibility was determined using an overdriving pacing protocol, and AF was defined as the occurrence of rapid and fragmented atrial electrograms with irregular AV-nodal conduction and ventricular rhythm for at least 1 s. To be counted as AF positive, a mouse had to exhibit AF in response to at least two out of three pacing trials. For *Kcna1*-null mice, the mean AF duration was determined by calculating the average elapsed time of all observed AF episodes. The

stimulation protocols used for intracardiac burst pacing are summarized in Supplemental Table S1.

Mouse RNA extraction, cDNA synthesis, and real-time PCR

Similarly aged Kv1.1-knockout mice (n = 5; 112 ± 5 days old) and wild-type control mice (n = 5; 121 ± 5 days old) were euthanized using isoflurane inhalation and their left atria quickly excised. The tissue was immediately placed in ice-cold TRIzol reagent, homogenized, and the total RNA extracted according to the manufacturer's protocol (Invitrogen, Carlsbad, CA, USA). Following resuspension in water, RNA samples were DNase treated using the DNA-*free* Kit (Applied Biosystems, Carlsbad, CA, USA). The quantity of total RNA was measured and the quality checked by agarose gel electrophoresis.

First-strand cDNA was synthesized from 250 ng of total RNA using the Phusion RT-PCR Kit with oligo(dT) primers (ThermoScientific, Waltham, MA, USA). Before proceeding to real-time PCR, the quality of cDNA and the tissue genotype was verified by 40 cycles of PCR amplification using primers specific for the *GAPDH* and *Kcna1* genes, followed by agarose gel electrophoresis. A 982-bp *GAPDH*-specific band was amplified using the following primers: forward, 5′-TGAAGGTCGGTGTGAACGGATTTGGC-3′; reverse, 5′-ATGTAGGCCATGAGGTCCACCAC-3′. A 710-bp *Kcna1*-specific band was amplified using the following primers: forward, 5′-GCATCGACAACACCACAGTC-3; reverse, 5′-CGGCGGCTGAGGTCACTGTCAGAGGCTAAGT-3′. The lack of *GAPDH* PCR products in –RT controls confirmed the absence of genomic DNA contamination, while the presence or absence of *Kcna1* amplicons confirmed the tissue genotype and verified the absence of *Kcna1* mRNA in knockouts.

To quantify the relative gene expression patterns in left atria of knockout and control animals, real-time RT-PCR of first strand cDNA was performed with TaqMan gene expression assays using the 7500 Real-Time PCR System (Applied Biosystems). TaqMan gene expression assays were designed and preoptimized by Applied Biosystems for the detection of *Kcna1* (Mm00439977_s1), *Kcna2* (Mm00434584_s1), *Kcna3* (Mm00434599_s1), *Kcna4* (Mm00445241_s1), *Kcna5* (Mm00524346_s1), *Kcna6* (Mm00496625_s1), *Kcna7* (Mm01197268_m1), *Kcnab1* (Mm00440017_m1), *Kcnab2* (Mm01260263_m1), *Kcnab3* (Mm01337146_m1), *col6a1* (Mm00487160_m1), and *Hprt1* (Mm00446968_m1). Each assay consisted of an unlabeled gene-specific PCR primer pair and a TaqMan probe with a fluorescent FAM dye label and a minor groove binder moiety on the 5′ end and a nonfluorescent quencher on the 3′ end. Individual PCRs were performed in triplicate using 100 ng of cDNA and TaqMan Gene Expression Master Mix (Applied Biosystems). No template and –RT reactions were included as negative controls to verify the absence of contamination leading to unwanted PCR amplification and detection. The reactions were cycled at 50 °C for 2 min, 95 °C for 10 min, and then 40 cycles of 95 °C for 15 s and 60 °C for 1 min. Spectral data were collected and analyzed with SDS 1.3 software (Applied Biosystems) using a manual threshold of 0.1, automatic baseline detection, and automatic outlier removal. The data were analyzed using the threshold cycle (C_t) relative quantification method [16]. *Hprt1* was used as a reference gene for normalization since it showed stable and reliable expression in our samples. *GAPDH* was also evaluated as a

reference gene but its expression was more variable than *Hprt1*, so it was excluded from the analysis. The C_t values were averaged and then used to calculate the expression levels relative to *Hprt1* using the formula $2^{-\Delta C_t}$ X 100, where $2^{-\Delta C_t}$ corresponds to the difference in the threshold cycle of the gene of interest versus *Hprt1*. In two instances, once for *Kcna6* and once for *Kcnab3* (both in wild-type samples), the assays failed to amplify across the entire triplicate, even when the experiment was repeated, likely due to extremely low levels of gene expression. In both cases, a value of zero was imputed for the $2^{-\Delta C_t}$ measurement for the given samples. In rare instances where triplicates produced only one successful replicate, the C_t value used for data analysis was derived from the single working reaction, assuming that the measurement was similar to the other biological replicates. Values for *Kcna1* levels in knockout tissue were imputed as zero since the TaqMan assay used for detection is uninformative in knockouts; the *Kcna1* assay is targeted to the 5′-UTR of the gene which is still present in knockouts despite the absence of the open reading frame. As stated above, all knockout tissues were verified to be negative for *Kcna1* mRNA using 40 cycles of RT-PCR followed by agarose gel electrophoresis.

Mouse histology

Whole hearts from 4- to 6-month-old mice were excised, submerged in 1 M KCl for 45–60 s, rinsed briefly in PBS, and then fixed in 10 % neutral buffered formalin for 24 h. Following fixation, hearts were embedded in paraffin, longitudinally sectioned (5 μm), and stained with Masson's trichrome for fibrosis. The percentage of fibrotic atrial tissue was quantified with Adobe Photoshop using previously described methods [8]. In brief, images were adjusted using the selective color command to intensify the contrast between reds and blues. The color range function was then used to generate histograms which counted the pixel area for each of the color components. The fraction of tissue fibrosis was then calculated by dividing the sum of the cyan and blue pixel areas by the total pixel area. For each animal, percentage fibrosis was estimated by averaging measurements from left and right atria in similarly oriented single longitudinal sections. Fibrosis percentages appeared similar between left and right atria for each genotype. For one knockout and one control animal, fibrosis was measured in only the left or right atria due to the loss of tissue during processing.

Cardiomyocyte isolation and expression analyses

C57BL/6 mice (3 months old) were used for cell isolation as described previously [15]. In brief, following isoflurane anesthesia, the heart was removed from mice. After dissecting, the heart was cannulated through the aorta and perfused on a Langendorff apparatus with 0 Ca^{2+} Tyrode, then 0 Ca^{2+} Tyrode containing 0.02 mg/mL Liberase TH Research Grade (Roche Applied Science, Penzberg, Germany) for 10–15 min at 37 °C. After digestion, atria and ventricle were separated and placed in KB solution (90 mmol/L KCl, 30 mmol/L K_2HPO_4, 5 mmol/L $MgSO_4$, 5 mmol/L pyruvic acid, 5 mmol/L β-hydroxybutyric acid, 5 mmol/L creatine, 20 mmol/L taurine, 10 mmol/L glucose, 0.5 mmol/L EGTA, 5 mmol/L HEPES; pH 7.2), then minced thoroughly and agitated gently, and filtered through a 210 μm mesh. The isolated myocytes were spun down at 800 rpm for 5 min. After removing supernatant, the cells were used immediately for expression analysis or stored at −80 °C for biochemical studies later.

Total RNA was isolated using Direct-zolTM RNA MiniPrep (Zymo Research, Irvine, CA, USA) according to the manufacturer's instructions. In column DNase I digestion was performed to remove DNA contamination. First-stand cDNA was synthesized from 300 ng of total RNA using iScript™ cDNA Synthesis Kit (Bio-Rad, Hercules, CA, USA). PCR was then performed as described above in "Mouse RNA extraction, cDNA synthesis, and real-time PCR" using the same primers and amplification protocol. Quantitative real-time PCR (qRT-PCR) was performed as previously reported with modifications [28]. Briefly, qRT-PCR was performed in triplicates with PerfeCTa® SYBR® Green FastMix (Quanta BioSciences, Inc., Gaithersburg, MD, USA) in 96-well plates using Mastercycler ep realplex (Eppendorf, Hamburg, Germany). The following program was run to amplify the products: (1) 95 °C for 5 min, (2) 45 cycles of 95 °C for 5 s, 60 °C for 10 s, 72 °C for 1 s, (3) melting curve ramp from 65 °C to 95 °C at 0.1 °C per second. mRNA expression levels were compared using the relative CT (cycle number) method after normalization to *Rpl7*. Primer sequences for *Kcna1* were the following: forward, 5′-GAGAATGCGGACGAGGCTTC-3′ and reverse, 5′-CCGGAGATGTTGATTACTACGC-3′. For *Rpl7*, the primers had the following sequence: forward, 5′GAAGCTCATCTATGAGAAGGC-3′ and reverse, 5′-AAGACGAAGGAGCTGCAGAAC-3′.

For immunocytochemistry, isolated myocytes were added to cover glasses coated with 20 μg/ml laminin in PBS for 30 min before fixation with 4 % formalin for 15 min. After washing with PBS 3 times, the myocytes were permeabilized with 0.1 % Triton X in PBS for 10 min, washed another 3 times with PBS, and blocked with 1 % normal goat serum (NGS) in PBS for 1 h. After blocking, the samples were incubated overnight at 4 °C with antibodies against Kv1.1 (K20/78, NeuroMab, Davis, CA, USA; 1:100) and JPH2 (custom-made [26]; 1:100) diluted in 1 % NGS and 1 % bovine serum albumin (BSA) in PBS. Next day, the cover glasses were washed with PBS 3 times and incubated with Alexa Fluor® 568 Goat Anti-Mouse IgG and Alexa Fluor® 488 Goat Anti-Rabbit IgG (#A11004, Invitrogen, Carlsbad, CA, USA; 1:2000 for both) in 1 % NGS/BSA in PBS for 1 h at room temperature. Afterward, the cover glasses were washed with PBS 3 times and mounted on glass slide with Vectashield media with DAPI (#H-1200, Vector Laboratories, Burlingame, CA, USA). Fluorescence images were taken with the Zeiss LSM510 confocal microscope (Jena, Germany).

Human tissue samples

Right atrial appendages were obtained from 32 patients in sinus rhythm (SR), 14 in paroxysmal AF (pAF) and 23 in chronic AF (cAF), undergoing open-heart surgery (Table 1). Experimental protocols were approved by the ethics committee of the Medical Faculty Mannheim, University of Heidelberg (#2011-216 N-MA) and performed in accordance with the Declaration of Helsinki. Each patient gave written informed consent. After excision, atrial appendages were used for either myocyte isolation (6 SR, 6 cAF) or snap-frozen in liquid-nitrogen for biochemical studies (26 SR, 14 pAF, 17 cAF patients).

Human RNA and protein biochemistry

RNA isolation, reverse-transcription and real-time PCR were performed as described [43]. For initial detection of *KCNA1* mRNA, cDNA was PCR-amplified using 35 cycles and

primers specific for the *KCNA1* gene, followed by agarose gel electrophoresis. A 232-bp *KCNA1*-specific band was amplified using the following primers: forward, 5′-CATCGTGGAAACGCTGTGTAT-3; reverse, 5′AACCCTTACCAAGCGGATGAC-3′. Commercial primers were used for real-time PCR detection of human *KCNA1* mRNA expression in patients (Hs00264798_s1, Life Technologies, Foster City, CA, USA). *KCNA1* mRNA expression was normalized to *HPRT1* (Hs01003267_m1; Life Technologies).

Protein levels of Kv1.1 (1:1000; rabbit polyclonal anti-Kv1.1; ARP34923_P050; Aviva Systems Biology, San Diego, CA, USA) were quantified by Western blotting and normalized to GAPDH (1:200,000; HyTest, Turku, Finland) as described [43]. Peroxidase-conjugated goat antirabbit (1:5000; Sigma-Aldrich, St. Louis, MO, USA) and goat anti-mouse (1:50,000; Sigma-Aldrich) were used as secondary antibodies and visualized by chemifluorescense (GE Healthcare, Chalifont St. Giles, UK). AIDA Image Analyzer Software (raytest, Straubenhardt, Germany) was used for analysis.

For immunocytochemistry, cells (from 3 patients in SR; 8 cells/patient) were fixed with paraformaldehyde (PFA; 2 %) for 15 min. After centrifugation at 750 rpm for 5 min, PFA was removed, the myocytes were washed, and PFA was neutralized with Glycin (0.1 M). Cells were then washed 3 times with phosphate-buffered saline (PBS) and permeabilized for 5 min with Triton X-100 (0.5 %) diluted in PBS. Cells were rinsed 3 times with PBS and then blocked with 1 % BSA in PBS. Myocytes were then labeled with the primary antibody (rabbit polyclonal anti-Kv1.1 (1:1000); ARP34923_P050; Aviva Systems Biology, San Diego, CA, USA), which was diluted in PBS containing 1 % BSA. After an overnight incubation at 4 °C, the myocytes were washed 3 times using 1 % BSA in PBS and then incubated with Fluorescein (FITC, excitation 488 nm, emission 520 nm) anti-rabbit IgG to reveal the Kv1.1 staining. After 3 successive 5-min washes using 1 % BSA in PBS, the cells were mounted with Mowiol medium. Images were acquired using a CAIRN Spinning Disk confocal microscope.

Patch-clamp experiments

Atrial myocytes were isolated using a standard protocol and were suspended in storage solution (mmol/L: KCl 20, KH_2PO4 10, glucose 10, K-glutamate 70, β-hydroxybutyrate 10, taurine 10, EGTA 10, albumin 1, pH = 7.4) [44]. Membrane currents were measured in whole-cell ruptured-patch configuration using voltage clamp. pClamp-Software V10.2 (Molecular Devices, Sunnyvale, USA) was used for data acquisition and analysis. Borosilicate glass microelectrodes had tip resistances of 2–5 MΩ when filled with pipette solution (mmol/L: EGTA 0.02, GTP-Tris 0.1, HEPES 10, K-aspartate 92, KCl 48, Mg-ATP 1, Na_2-ATP 4; pH = 7.2). Seal resistances were 4–8 GΩ. Series resistance and cell capacitance were compensated. The series resistance was kept below 10 MΩ and was compensated by at least 50 %. With a current amplitude of 1 nA, the potential for error amounted to <5 mV. To control for myocyte-size variability, currents are expressed as densities (pA/pF). Myocytes were superfused at 37 °C with a bath solution containing (mmol/L): $CaCl_2$ 2, glucose 10, HEPES 10, KCl 4, $MgCl_2$ 1, NaCl 140, probenecid 2; pH = 7.4. $I_{Ca,L}$ was blocked by adding $CdCl_2$ (0.3 mmol/L) to the bath solution. Drugs were applied via a rapidsolution exchange system (ALA Scientific Instruments, Farmingdale,

USA). Dendrotoxin-K (10 nmol/L; Alomone Labs, Jerusalem, Israel) was used to block Kv1.1 currents [31].

Statistical analysis

Differences between group means for continuous data were compared by unpaired two-tailed Student's *t* test. Differences between mean mRNA levels in mouse ventricular and atrial myocytes were compared using a paired *t* test. Categorical data were analyzed with Fisher's exact test. Data are mean ± SEM. $P < 0.05$ was considered statistically significant. In statistical comparisons of myocyte electrophysiology data, patients may contribute more than one observation to each sub-analysis suggesting that observations are not necessarily independent. Within-patient correlations were not taken into account in statistical comparisons due to the low sample size.

Results

Increased susceptibility to pacing-induced AF in *Kcna1*-null mice

In our previous studies using video electroencephalography (EEG) combined with ECG, unequivocal spontaneous AF was not identified in the ambulatory ECGs of *Kcna1*-null mice [11]. To test for AF inducibility, *Kcna1*-null mice (age 4.0 ± 0.3 months) and WT controls (age 4.1 ± 0.3 months) were subjected to intracardiac right atrial burst pacing stimulation. Simultaneous surface electrocardiograms (ECG) and intracardiac atrial and ventricular electrograms were recorded to monitor the occurrence of atrial arrhythmias (Fig. 1a). AF was characterized by the combination of a lack of P waves combined with the presence of irregular RR intervals in lead I of the surface ECG (Fig. 1b). Burst pacing induced AF more frequently in *Kcna1*-null mice (40 %, 5 of 12) than WT mice (0 %, 0 of 10; $P < 0.05$; Fig. 1c). The average duration of AF episodes in *Kcna1*-null mice was 8.0 ± 2.9 s, and normal sinus rhythm always resumed spontaneously. Experiments using ventricular burst pacing protocols did not show obvious differences in ventricular arrhythmia susceptibility between genotypes.

Baseline recordings during anesthesia did not reveal any significant differences in surface ECG characteristics between *Kcna1*-null and WT animals, except for slight but significant shortening of the QRS interval in null mice (6.9 ± 0.2 ms in *Kcna1*-null mice versus 7.8 ± 0.4 ms in WT; $P < 0.05$; Table 2). Cardiac conduction system properties also appeared unaltered, since no significant differences were found in the sinus node recovery time, right atrial effective refractory period, and atrioventricular node effective refractory period (Table 2). The lack of obvious baseline changes in atrioventricular node function and sinus cycle length in *Kcna1*-null mice suggests a possible neural origin for the increased frequency of AV conduction blocks found previously in this model; however, autonomic inputs remain intact in our preparations and could mask latent cardiac-intrinsic differences. Heart mass was compared between genotypes to rule out any effects due to cardiac hypertrophy or remodeling. Hearts of *Kcna1*-null mice tended to be larger as measured by absolute heart mass and heart mass-to-body mass ratio, but this trend did not reach significance (Table 2).

Minimal Kv1 channel and fibrotic structural remodeling in atria of *Kcna1*-null mice

Next, mRNA expression analysis was used to determine whether the increased AF susceptibility in *Kcna1*-null mice was potentially caused by compensatory expression changes in related Kv1.x potassium channel α-subunits, such as *Kcna5* which has been linked to AF [25, 52]. Real-time PCR was performed on atrial tissue from *Kcna1*-null and WT mice to compare mRNA expression levels for the genes *Kcna1-7* and *Kcnab1-3*, which encode the Kv1.1–Kv1.7 pore-forming α-subunits and their associated Kvbeta1-3 accessory β-subunits, respectively. In WT mice, measurable expression levels were detected for all seven α-subunits and all three β-subunits. Among the α-subunits, *Kcna5* was expressed at the highest level followed by *Kcna4* and *Kcna7*, while *Kcna1, Kcna2, Kcna3*, and *Kcna6* were expressed at similarly low levels (*Kcna5* ≫ *Kcna4* > *Kcna7* > *Kcna1* ≈ *Kcna2* ≈ *Kcna3* ≈ *Kcna6*). There were no substantial compensatory changes in gene expression levels for the Kv1.2–Kv1.7 α-subunits in *Kcna1*-null mice (age 3.7 ± 0.2 months; Fig. 2a). Among the β-subunits, all were expressed at similarly low levels, and the *Kcnab1* subunit showed a modest but significant 31 % decrease ($P < 0.05$). However, the overall lack of major Kv1.x channel subunit remodeling suggests that the observed increase in AF susceptibility is likely directly related to Kv1.1 deficiency and not attributable to compensatory dysregulation of related Kv1 subunits.

Since fibrotic structural remodeling can provide a substrate conducive to AF, the hearts of *Kcna1*-null mice were examined for evidence of increased fibrillar collagen deposits. First, transcript levels of the *collagen, type VI, alpha 1* (*col6a1*) gene were measured as an indicator of fibrosis. *Col6a1* expression levels were significantly increased by more than 50 % in *Kcna1*-null atria relative to WT controls (Fig. 2b; $P < 0.05$). To determine whether this increase in collagen mRNA correlated with an increase in fibrosis, Masson's trichrome staining of atria was performed to label collagen fibers (Fig. 2c). Quantification of the percentage of atrial fibrotic tissue showed that *Kcna1*-null hearts (1.9 ± 0.7 %) tended to have about twice as much collagen as age-matched wild-type controls (1.0 ± 0.6 %), but the results were highly variable between animals and did not reach statistical significance (Fig. 2d; $P = 0.35$). Thus, atrial arrhythmogenesis in *Kcna1*-null hearts is not clearly correlated with increased atrial fibrosis.

Kv1.1 channels are expressed in isolated mouse cardiomyoctes

To verify that *Kcna1* is expressed in cardiomyocytes and not only intracardiac neurons, individual atrial and ventricular myocytes were isolated from mouse heart and analyzed for Kv1.1 mRNA and protein. RT-PCR revealed the unequivocal presence of Kv1.1 mRNA in isolated atrial myocytes, but ventricular transcripts were below the limit of detection (Fig. 3a). Using the more sensitive technique of real-time PCR to quantify relative mRNA levels, Kv1.1 transcripts were detected in both atrial and ventricular cells, but the abundance in atrial myocytes was about tenfold higher (Fig. 3b; $P = 0.07$). To determine whether *Kcna1* expression could be detected at the protein level in individual mouse myocytes, immunocytochemistry was performed. Kv1.1 immunoreactivity was observed in both atrial and ventricular myocytes (Fig. 3c, d); however, the Kv1.1-positive ventricular staining appeared much less intense overall. Importantly, Kv1.1 immunoreactivity was absent in

cardiomyocytes from *Kcna1*-null mice demonstrating the specificity of the antibody labeling (Fig. 3c, d).

Kv1.1 channels are expressed in human heart and upregulated in chronic AF

The increased AF susceptibility in the *Kcna1*-null mouse model suggests that Kv1.1 channels may play a role in AF pathophysiology in patients. However, the expression of *KCNA1* has never been demonstrated in human heart nor associated with arrhythmia in humans. Using RT-PCR, *KCNA1* mRNA was detected in human atrial samples confirming its presence in human cardiac tissue for the first time (Fig. 4a). Since *KCNA1* transcripts were measurable in human atria, mRNA levels of *KCNA1* were quantified in patients with paroxysmal (pAF) and chronic AF (cAF) to look for disease-associated alterations. Using real-time RT-PCR, *KCNA1* mRNA expression levels were found to be significantly increased in pAF patients but not in cAF individuals relative to controls in sinus rhythm (SR) (Fig. 4b; $P < 0.0005$).

Since transcription levels do not always accurately reflect the amount of translated protein, western blots were performed to measure Kv1.1 subunit abundance in patients and controls. Immunoblots of atrial tissue revealed the presence of detectable amounts of Kv1.1 protein in human heart for the first time (Fig. 4c, d). Quantification of Kv1.1 subunit levels revealed no change in Kv1.1 protein levels in pAF patients (P = 0.804) but an unexpected and significant 75 % increase in Kv1.1 protein levels in cAF patients compared to SR controls (Fig. 4c, d; $P < 0.05$). Kv1.1 protein appeared similarly increased in cAF patients with and without valvular heart disease (Supplementary Figure 1). To verify that human Kv1.1 protein expression was associated with cardiomyocytes and not with other cell types, immunocytochemistry of isolated human atrial myocytes was performed revealing significant myocyte-specific Kv1.1 immunoreactivity (Fig. 5). The substantial upregulation of Kv1.1 subunits in the atria of cAF patients, but not pAF, suggests that the channels undergo expression remodeling that may contribute to AF pathophysiology and be a potential determinant of the transition to maintained AF.

Kv1.1 subunits form functional channels in human atrial myocytes

Having detected Kv1.1 subunits in human atria, patchclamp recordings were performed utilizing a Kv1.1-specific inhibitor, dendrotoxin-K (DTX-K), to determine whether the channels make a functional contribution to human cardiac currents [31]. Following enzymatic isolation of human myocytes from right atrial appendages of patients in SR, whole-cell voltage clamp recordings were performed to measure outward membrane currents using a voltage step protocol composed of brief one-second depolarizations from −60 mV to +50 mV at 0.1 Hz to activate outward K^+ currents (Fig. 6a). In the presence of DTX-K to selectively block Kv1.1 subunits, the peak and late outward current amplitudes were significantly reduced by about 20 and 10 %, respectively (Fig. 6b, c; $P < 0.01$ and 0.05, respectively). This DTX-K-sensitive component of the outward current is indicative of a small but significant contribution by Kv1.1-containing channels to the total repolarizing K^+ current in human atrial myocytes. Thus, Kv1.1 channels are not only present in human heart, but they are also functional and contribute to atrial repolarization.

Kv1.1-associated currents are increased in cAF patients

To determine if the observed cAF-associated increase in Kv1.1 protein levels corresponds with an increase in Kv1.1-associated currents, the DTX-K-sensitive component was then measured in atrial myocytes isolated from patients with cAF. Membrane capacitance was not significantly different between SR and cAF myocytes suggesting similar cell sizes in each group ($P = 0.59$; Supplementary Figure 2). Myocytes from patients with cAF showed a slight reduction in K^+-current amplitudes, which did not reach the level of statistical significance (Fig. 6a). However, both the peak and late components of the DTX-K-sensitive current showed a significant two- to three-fold increase compared to SR (Fig. 6b–d; $P < 0.05$ and 0.01 at peak and late current levels, respectively). To further characterize our patient cohort, $I_{Ca,L}$ was measured in myocytes from SR and cAF patients as a major hallmark of electrical remodeling. Consistent with previous reports, $I_{Ca,L}$ was significantly reduced by about 50 % in cAF myocytes compared to SR (Supplementary Figure 3) [46]. The substantial increase in DTX-K-sensitive current in cAF patients, coupled with increased *KCNA1* expression, suggests that Kv1.1 channels undergo molecular and electrical remodeling, which may contribute to the pathomechanisms of persistent AF.

Discussion

Traditionally, Kv1.1 channels have been regarded as brain-specific channels with little to no cardiac expression but our evidence suggests that this paradigm needs to be reconsidered. Here RT-PCR, western blotting, and immunocytochemistry demonstrate the presence of Kv1.1 channels in human atria; the first time they have been reported in human heart. Prior studies found Kv1.1 transcripts in mouse and rat hearts using Northern blotting but the abundance was so low that they were thought to result from sample contamination by neural tissues [18, 30]. More recently, newer RT-PCR-based methods with higher sensitivity reproducibly detected Kv1.1 transcripts in mouse heart, especially in nodal regions where the gene appears to be expressed at relatively high levels [11, 12, 14, 20]. This work verifies the presence of Kv1.1 mRNA in mouse atria, albeit at apparently low abundance. Importantly, Kv1.1 mRNA was detected in isolated mouse cardiomyocytes for the first time in this study, demonstrating that Kv1.1 expression in cardiac tissue cannot be solely attributed to contamination by neural cells. Interestingly, Kv1.1 transcripts showed higher expression in atrial myocytes than ventricular, similar to what has been reported for Kv1.5 subunits [39]. Furthermore, at the protein level, this study provides the first evidence of Kv1.1 immunoreactivity in individual cardiomyocytes. In mice, the Kv1.1-positive labeling in atrial myocytes appeared predominantly intracellular, whereas the weaker staining in ventricular myocytes showed clustering in a pattern consistent with transverse tubules, as revealed by co-labeling with the t-tubule marker protein Junctophilin-2. The Kv1.1 immunoreactivity in human atrial myocytes was similar to that seen in mice with a predominantly intracellular staining pattern, as well as striations consistent with localization at Z-lines. The mostly intracellular Kv1.1 staining pattern in atrial myocytes may reflect a relative abundance of the channel in intracellular pools awaiting membrane insertion in response to some physiological trigger. For example, atrial Kv1.5 channels are dynamically recruited to the membrane from submembranous pools in response to high sheer stress or

cholesterol depletion [1, 3]. However, further experimentation will be required to determine whether Kv1.1 channels undergo similar trafficking mechanisms.

Our identification of DTX-K-sensitive outward currents in human atrial myocytes suggests that Kv1.1 channels make a previously unrecognized contribution to membrane repolarization during the atrial action potential. Biochemical and electrophysiological studies have repeatedly demonstrated the exquisitely strict specificity of DTX-K for inhibition of only Kv1.1 subunits [31, 48, 49]. The two primary voltage-gated potassium currents in human atrial myocytes are the fast transient outward current ($I_{to,f}$) and the ultra-rapid delayed rectifier potassium current (I_{Kur}), which are encoded by Kv4.3 and Kv1.5 α-subunits, respectively. Since DTX-K reduced the peak and late outward currents, we predict that Kv1.1 channels make a small but significant contribution to $I_{to,f}$ and I_{Kur}. Of note, human atrial myocytes exhibit a substantial late outward I_{Kur} current component of unknown molecular origin and composition that is characterized as being non-inactivating, insensitive to the Kv1.5-blocker AVE0118, and increased in cAF myocytes relative to SR [6, 41]. The DTX-K-sensitive late currents recorded here fit the profile of this unidentified non-inactivating, AVE0118-insensitive current component of I_{Kur}, suggesting that it may be encoded by Kv1.1 channels. In addition to $I_{to,f}$ and I_{Kur}, human atrial myocytes also exhibit a rapidly activating and inactivating current (I_{Kr}) and a slowly activating current (I_{Ks}), mediated by hERG1 and KCNQ1 channels, respectively, but they are much smaller outward potassium currents relative to $I_{to,f}$ and I_{Kur} [2, 24, 33, 34, 40]. Whether Kv1.1 channels contribute to I_{Kr} or I_{Ks} cannot be inferred from this work, since the myocyte isolation protocol largely destroys the I_{Kr} current and the voltage step duration is too short to accurately discriminate classical I_{Ks}. In summary, human atrial myocytes exhibit significant DTX-K-sensitive peak and late outward currents that may represent a previously unrecognized contribution by Kv1.1 channels to $I_{to,f}$ and I_{Kur}.

Elucidation of the subunit stoichiometry of the functional cardiac Kv1.1 channel may help resolve the identity and role of the Kv1.1-associated cardiac current in the atrial action potential. The kinetics and gating properties of Kv1-mediated currents are determined by their associated α- and β-subunit composition. For example, Kv1.4 α-subunits and Kvβ1 accessory subunits confer fast N-type inactivation via the presence of ball domains, whereas Kv1.6 α-subunits possess N-type inactivation prevention (NIP) domains that can neutralize inactivation gating [27, 32, 38]. Studies in brain show that Kv1.1 α-subunits preferentially form functional heterotetrameric assemblies with Kv1.2 or Kv1.4 and sometimes Kv1.6 [49]. Future biochemical analyses will be required to determine which Kv1 α- and β-subunit combinations exist in heart, and what their respective functional roles might be.

The significant increase in DTX-K-sensitive currents in cAF myocytes with concomitant upregulation of Kv1.1 protein levels suggests that Kv1.1 channels may contribute to electrical remodeling in cAF. The transition from paroxysmal to persistent AF is facilitated by atrial remodeling of ion channels at the level of expression and electrophysiological properties [9, 13, 23, 42, 45]. These AF-related electrical adaptations generally promote shortening of the atrial action potential and blunting of the atrial effective refractory period, which increases vulnerability to AF by providing a proarrhythmogenic substrate prone to premature beats [9, 23]. In AF patients, Kv4.3 channel mRNA and protein are

downregulated leading to a 60 % decrease in I_{to}, which is thought to indirectly increase the upstroke velocity of the atrial action potential leading to augmented wave propagation that promotes maintenance of AF [5, 51]. Remodeling has also been reported for the atrial voltage-gated K^+ channels hERG1, Kv1.5 and KCNQ1, but their expression changes have either been inconsistent or not correlated with corresponding changes in atrial currents [23]. The concurrent increase in Kv1.1 protein expression and Kv1.1-mediated outward currents provides one of the first examples of cAF-associated upregulation remodeling of a voltage-gated potassium channel. Interestingly, we did not find corresponding increases in *KCNA1* mRNA levels in cAF atria suggesting the influence of post-transcriptional modifications similar to Kv1.5 channels which also exhibit a discordance between mRNA and protein levels in cAF patients [4, 5]. The augmentation of Kv1.1 protein expression and currents is consistent with the reduced action potential durations characteristic of AF, but whether these are primary causative changes or secondary compensations remains to be tested.

The increased incidence of inducible AF in Kv1.1-deficient mice suggests that *Kcna1* may be a new candidate gene for AF susceptibility; however, the overexpression of Kv1.1 channels in cAF patients appears contradictory to this notion. Some of this discrepancy could be related to inter-species differences in atrial physiology and channel expression between mice and humans [17]. Loss-of-function mutations in the related voltage-gated potassium channel *KCNA5* unexpectedly lead to AF by an atypical mechanism involving decreased I_{Kur} which leads to a predisposition for atrial action potential prolongation and early after-depolarizations [25, 52]. Kv1.1-deficiency may cause similar complex AF-promoting alterations in atrial function; however, in humans *KCNA1* gene variants have yet to be associated with AF. Determination of whether the upregulation of Kv1.1 channels in cAF patients is causative for AF or a compensatory mechanism is necessary to resolve the role of Kv1.1 channels in AF. If it is compensatory, Kv1.1 currents would be expected to oppose AF and their absence would be expected to promote AF as seen in our mouse model. Additional studies will be required to dissect the exact contribution of Kv1.1 currents to action potential duration and AF susceptibility in mice and humans, especially given the complex relationship between modification of outward potassium currents and action potential morphology [7].

Supplementary Material

Refer to Web version on PubMed Central for supplementary material.

Acknowledgments

The authors thank Ramona Nagel and Katrin Kupser for excellent technical assistance. This work was supported by grants from the National Institutes of Health (HL107641 to EG; HL089598, HL091947, and HL117641 to X.H.T.W.; NS076916 to J.L.N.), the Muscular Dystrophy Association (X.H.T.W.), American Heart Association (13EIA14560061 to X.H.T.W.), the Deutsche Forschungsgemeinschaft (Do 769/1-1-3 to D.D.), the German Federal Ministry of Education and Research through DZHK (German Centre for Cardiovascular Research to D.D.), the European Union through the European Network for Translational Research in Atrial Fibrillation (EUTRAF, FP7-HEALTH-2010, large-scale integrating project, Proposal No. 261057 to D.D), and Fondation Leducq (‘Alliance for CaMKII Signaling in Heart’ to X.H.T.W. and ‘European North-American Atrial Fibrillation Research Alliance’ to D.D.).

References

1. Balse E, El-Haou S, Dillanian G, Dauphin A, Eldstrom J, Fedida D, Coulombe A, Hatem SN. Cholesterol modulates the recruitment of Kv1.5 channels from Rab11-associated recycling endosome in native atrial myocytes. Proc Natl Acad Sci. 2009; 106:14681–14686. [PubMed: 19706553]
2. Barhanin J, Lesage F, Guillemare E, Fink M, Lazdunski M, Romey G. K(V)LQT1 and lsK (minK) proteins associate to form the I(Ks) cardiac potassium current. Nature. 1996; 384:78–80. [PubMed: 8900282]
3. Boycott HE, Barbier CSM, Eichel CA, Costa KD, Martins RP, Louault F, Dilanian G, Coulombe A, Hatem SN, Balse E. Shear stress triggers insertion of voltage-gated potassium channels from intracellular compartments in atrial myocytes. Proc Natl Acad Sci. 2013; 110:E3955–E3964. [PubMed: 24065831]
4. Brundel BJ, Van Gelder IC, Henning RH, Tieleman RG, Tuinenburg AE, Wietses M, Grandjean JG, Van Gilst WH, Crijns HJ. Ion channel remodeling is related to intraoperative atrial effective refractory periods in patients with paroxysmal and persistent atrial fibrillation. Circulation. 2001; 103:684–690. [PubMed: 11156880]
5. Brundel BJ, Van Gelder IC, Henning RH, Tuinenburg AE, Wietses M, Grandjean JG, Wilde AA, Van Gilst WH, Crijns HJ. Alterations in potassium channel gene expression in atria of patients with persistent and paroxysmal atrial fibrillation: differential regulation of protein and mRNA levels for K+ channels. J Am Coll Cardiol. 2001; 37:926–932. [PubMed: 11693772]
6. Christ T, Wettwer E, Voigt N, Hála O, Radicke S, Matschke K, Várro A, Dobrev D, Ravens U. Pathology-specific effects of the IKur/Ito/IK, ACh blocker AVE0118 on ion channels in human chronic atrial fibrillation. Br J Pharmacol. 2008; 154:1619–1630. [PubMed: 18536759]
7. Courtemanche M, Ramirez RJ, Nattel S. Ionic targets for drug therapy and atrial fibrillation-induced electrical remodeling: insights from a mathematical model. Cardiovasc Res. 1999; 42:477–489. [PubMed: 10533583]
8. Dahab GM, Kheriza MM, El-Beltagi HM, Fouda A-MM, El-Din OAS. Digital quantification of fibrosis in liver biopsy sections: description of a new method by Photoshop software. J Gastroenterol Hepatol. 2004; 19:78–85. [PubMed: 14675247]
9. Dobrev D, Ravens U. Remodeling of cardiomyocyte ion channels in human atrial fibrillation. Basic Res Cardiol. 2003; 98:137–148. [PubMed: 12883831]
10. Glasscock E, Qian J, Kole MJ, Noebels JL. Transcompartmental reversal of single fibre hyperexcitability in juxtaparanodal Kv1.1-deficient vagus nerve axons by activation of nodal KCNQ channels. J Physiol. 2012; 590:3913–3926. [PubMed: 22641786]
11. Glasscock E, Yoo JW, Chen TT, Klassen TL, Noebels JL. Kv1.1 potassium channel deficiency reveals brain-driven cardiac dysfunction as a candidate mechanism for sudden unexplained death in epilepsy. J Neurosci. 2010; 30:5167–5175. [PubMed: 20392939]
12. Harrell MD, Harbi S, Hoffman JF, Zavadil J, Coetzee WA. Large-scale analysis of ion channel gene expression in the mouse heart during perinatal development. Physiol Genomics. 2007; 28:273–283. [PubMed: 16985003]
13. Heijman J, Dobrev D. Irregular rhythm and atrial metabolism are key for the evolution of proarrhythmic atrial remodeling in atrial fibrillation. Basic Res Cardiol. 2015; 110:498.
14. Leoni A-L, Marionneau C, Demolombe S, Le Bouter S, Mangoni ME, Escande D, Charpentier F. Chronic heart rate reduction remodels ion channel transcripts in the mouse sinoatrial node but not in the ventricle. Physiol Genomics. 2005; 24:4–12. [PubMed: 16219869]
15. Li N, Wang T, Wang W, Cutler MJ, Wang Q, Voigt N, Rosenbaum DS, Dobrev D, Wehrens XHT. Inhibition of CaMKII phosphorylation of RyR2 prevents induction of atrial fibrillation in FKBP12.6 knockout mice. Circ Res. 2012; 110:465–470. [PubMed: 22158709]
16. Livak KJ, Schmittgen TD. Analysis of relative gene expression data using real-time quantitative PCR and the 2(-Delta Delta C(T)) Method. Methods San Diego Calif. 2001; 25:402–408.
17. London B. Cardiac arrhythmias: from (transgenic) mice to men. J Cardiovasc Electrophysiol. 2001; 12:1089–1091. [PubMed: 11573703]

18. London B, Guo W, Pan Xh, Lee JS, Shusterman V, Rocco CJ, Logothetis DA, Nerbonne JM, Hill JA. Targeted replacement of KV1.5 in the mouse leads to loss of the 4-aminopyridinesensitive component of I(K, slow) and resistance to drug-induced qt prolongation. Circ Res. 2001; 88:940–946. [PubMed: 11349004]
19. Mahida S, Lubitz SA, Rienstra M, Milan DJ, Ellinor PT. Monogenic atrial fibrillation as pathophysiological paradigms. Cardiovasc Res. 2011; 89:692–700. [PubMed: 21123219]
20. Marionneau C, Couette B, Liu J, Li H, Mangoni ME, Nargeot J, Lei M, Escande D, Demolombe S. Specific pattern of ionic channel gene expression associated with pacemaker activity in the mouse heart. J Physiol. 2005; 562:223–234. [PubMed: 15498808]
21. Nattel S. New ideas about atrial fibrillation 50 years on. Nature. 2002; 415:219–226. [PubMed: 11805846]
22. Nattel S, Burstein B, Dobrev D. Atrial remodeling and atrial fibrillation: mechanisms and implications. Circ Arrhythm Electrophysiol. 2008; 1:62–73. [PubMed: 19808395]
23. Nattel S, Maguy A, Le Bouter S, Yeh Y-H. Arrhythmogenic ion-channel remodeling in the heart: heart failure, myocardial infarction, and atrial fibrillation. Physiol Rev. 2007; 87:425–456. [PubMed: 17429037]
24. Nerbonne JM, Kass RS. Molecular physiology of cardiac repolarization. Physiol Rev. 2005; 85:1205–1253. [PubMed: 16183911]
25. Olson TM, Alekseev AE, Liu XK, Park S, Zingman LV, Bienengraeber M, Sattiraju S, Ballew JD, Jahangir A, Terzic A. Kv1.5 channelopathy due to KCNA5 loss-of-function mutation causes human atrial fibrillation. Hum Mol Genet. 2006; 15:2185–2191. [PubMed: 16772329]
26. Van Oort RJ, Garbino A, Wang W, Dixit SS, Landstrom AP, Gaur N, De Almeida AC, Skapura DG, Rudy Y, Burns AR, Ackerman MJ, Wehrens XHT. Disrupted junctional membrane complexes and hyperactive ryanodine receptors after acute junctophilin knockdown in mice. Circulation. 2011; 123:979–988. [PubMed: 21339484]
27. Rettig J, Heinemann SH, Wunder F, Lorra C, Parcej DN, Dolly JO, Pongs O. Inactivation properties of voltage-gated K+ channels altered by presence of beta-subunit. Nature. 1994; 369:289–294. [PubMed: 8183366]
28. Reynolds JO, Chiang DY, Wang W, Beavers DL, Dixit SS, Skapura DG, Landstrom AP, Song L-S, Ackerman MJ, Wehrens XHT. Junctophilin-2 is necessary for T-tubule maturation during mouse heart development. Cardiovasc Res. 2013; 100:44–53. [PubMed: 23715556]
29. Robbins CA, Tempel BL. Kv1.1 and Kv1.2: similar channels, different seizure models. Epilepsia. 2012; 53(Suppl 1):134–141.
30. Roberds SL, Tamkun MM. Cloning and tissue-specific expression of five voltage-gated potassium channel cDNAs expressed in rat heart. Proc Natl Acad Sci USA. 1991; 88:1798–1802. [PubMed: 1705709]
31. Robertson B, Owen D, Stow J, Butler C, Newland C. Novel effects of dendrotoxin homologues on subtypes of mammalian Kv1 potassium channels expressed in Xenopus oocytes. FEBS Lett. 1996; 383:26–30. [PubMed: 8612784]
32. Roeper J, Sewing S, Zhang Y, Sommer T, Wanner SG, Pongs O. NIP domain prevents N-type inactivation in voltage-gated potassium channels. Nature. 1998; 391:390–393. [PubMed: 9450755]
33. Sanguinetti MC, Curran ME, Zou A, Shen J, Spector PS, Atkinson DL, Keating MT. Coassembly of K(V)LQT1 and minK (IsK) proteins to form cardiac I(Ks) potassium channel. Nature. 1996; 384:80–83. [PubMed: 8900283]
34. Sanguinetti MC, Jiang C, Curran ME, Keating MT. A mechanistic link between an inherited and an acquired cardiac arrhythmia: HERG encodes the IKr potassium channel. Cell. 1995; 81:299–307. [PubMed: 7736582]
35. Sinner MF, Ellinor PT, Meitinger T, Benjamin EJ, Kääb S. Genome-wide association studies of atrial fibrillation: past, present, and future. Cardiovasc Res. 2011; 89:701–709. [PubMed: 21245058]
36. Smart SL, Lopantsev V, Zhang CL, Robbins CA, Wang H, Chiu SY, Schwartzkroin PA, Messing A, Tempel BL. Deletion of the K(V)1.1 potassium channel causes epilepsy in mice. Neuron. 1998; 20:809–819. [PubMed: 9581771]

37. Sood S, Chelu MG, van Oort RJ, Skapura D, Santonastasi M, Dobrev D, Wehrens XHT. Intracellular calcium leak due to FKBP12.6 deficiency in mice facilitates the inducibility of atrial fibrillation. Heart Rhythm. 2008; 5:1047–1054. [PubMed: 18598963]
38. Stühmer W, Ruppersberg JP, Schröter KH, Sakmann B, Stocker M, Giese KP, Perschke A, Baumann A, Pongs O. Molecular basis of functional diversity of voltage-gated potassium channels in mammalian brain. EMBO J. 1989; 8:3235–3244. [PubMed: 2555158]
39. Tamkun MM, Knoth KM, Walbridge JA, Kroemer H, Roden DM, Glover DM. Molecular cloning and characterization of two voltage-gated K+ channel cDNAs from human ventricle. FASEB J Off Publ Fed Am Soc Exp Biol. 1991; 5:331–337.
40. Trudeau MC, Warmke JW, Ganetzky B, Robertson GA. HERG, a human inward rectifier in the voltage-gated potassium channel family. Science. 1995; 269:92–95. [PubMed: 7604285]
41. Turnow K, Metzner K, Cotella D, Morales MJ, Schaefer M, Christ T, Ravens U, Wettwer E, Kämmerer S. Interaction of DPP10a with Kv4.3 channel complex results in a sustained current component of human transient outward current Ito. Basic Res Cardiol. 2015; 110:5. [PubMed: 25600224]
42. Voigt N, Heijman J, Wang Q, Chiang DY, Li N, Karck M, Wehrens XHT, Nattel S, Dobrev D. Cellular and molecular mechanisms of atrial arrhythmogenesis in patients with paroxysmal atrial fibrillation. Circulation. 2014; 129:145–156. [PubMed: 24249718]
43. Voigt N, Li N, Wang Q, Wang W, Trafford AW, Abu-Taha I, Sun Q, Wieland T, Ravens U, Nattel S, Wehrens XHT, Dobrev D. Enhanced sarcoplasmic reticulum Ca2+ leak and increased Na+ -Ca2+ exchanger function underlie delayed after depolarizations in patients with chronic atrial fibrillation. Circulation. 2012; 125:2059–2070. [PubMed: 22456474]
44. Voigt N, Makary S, Nattel S, Dobrev D. Voltage-clamp-based methods for the detection of constitutively active acetylcholinegated I(K, ACh) channels in the diseased heart. Methods Enzymol. 2010; 484:653–675. [PubMed: 21036255]
45. Voigt N, Trausch A, Knaut M, Matschke K, Varró A, Van Wagoner DR, Nattel S, Ravens U, Dobrev D. Left-to-right atrial inward rectifier potassium current gradients in patients with paroxysmal versus chronic atrial fibrillation. Circ Arrhythm Electrophysiol. 2010; 3:472–480. [PubMed: 20657029]
46. Van Wagoner DR, Pond AL, Lamorgese M, Rossie SS, McCarthy PM, Nerbonne JM. Atrial L-type Ca2+ currents and human atrial fibrillation. Circ Res. 1999; 85:428–436. [PubMed: 10473672]
47. Wakili R, Voigt N, Kääb S, Dobrev D, Nattel S. Recent advances in the molecular pathophysiology of atrial fibrillation. J Clin Invest. 2011; 121:2955–2968. [PubMed: 21804195]
48. Wang FC, Bell N, Reid P, Smith LA, McIntosh P, Robertson B, Dolly JO. Identification of residues in dendrotoxin K responsible for its discrimination between neuronal K+ channels containing Kv1.1 and 1.2 alpha subunits. Eur J Biochem FEBS. 1999; 263:222–229.
49. Wang FC, Parcej DN, Dolly JO. Alpha subunit compositions of Kv1.1-containing K+ channel subtypes fractionated from rat brain using dendrotoxins. Eur J Biochem FEBS. 1999; 263:230–237.
50. Wijffels MC, Kirchhof CJ, Dorland R, Allessie MA. Atrial fibrillation begets atrial fibrillation. A study in awake chronically instrumented goats. Circulation. 1995; 92:1954–1968. [PubMed: 7671380]
51. Workman AJ, Kane KA, Rankin AC. The contribution of ionic currents to changes in refractoriness of human atrial myocytes associated with chronic atrial fibrillation. Cardiovasc Res. 2001; 52:226–235. [PubMed: 11684070]
52. Yang Y, Li J, Lin X, Yang Y, Hong K, Wang L, Liu J, Li L, Yan D, Liang D, Xiao J, Jin H, Wu J, Zhang Y, Chen Y-H. Novel KCNA5 loss-of-function mutations responsible for atrial fibrillation. J Hum Genet. 2009; 54:277–283. [PubMed: 19343045]

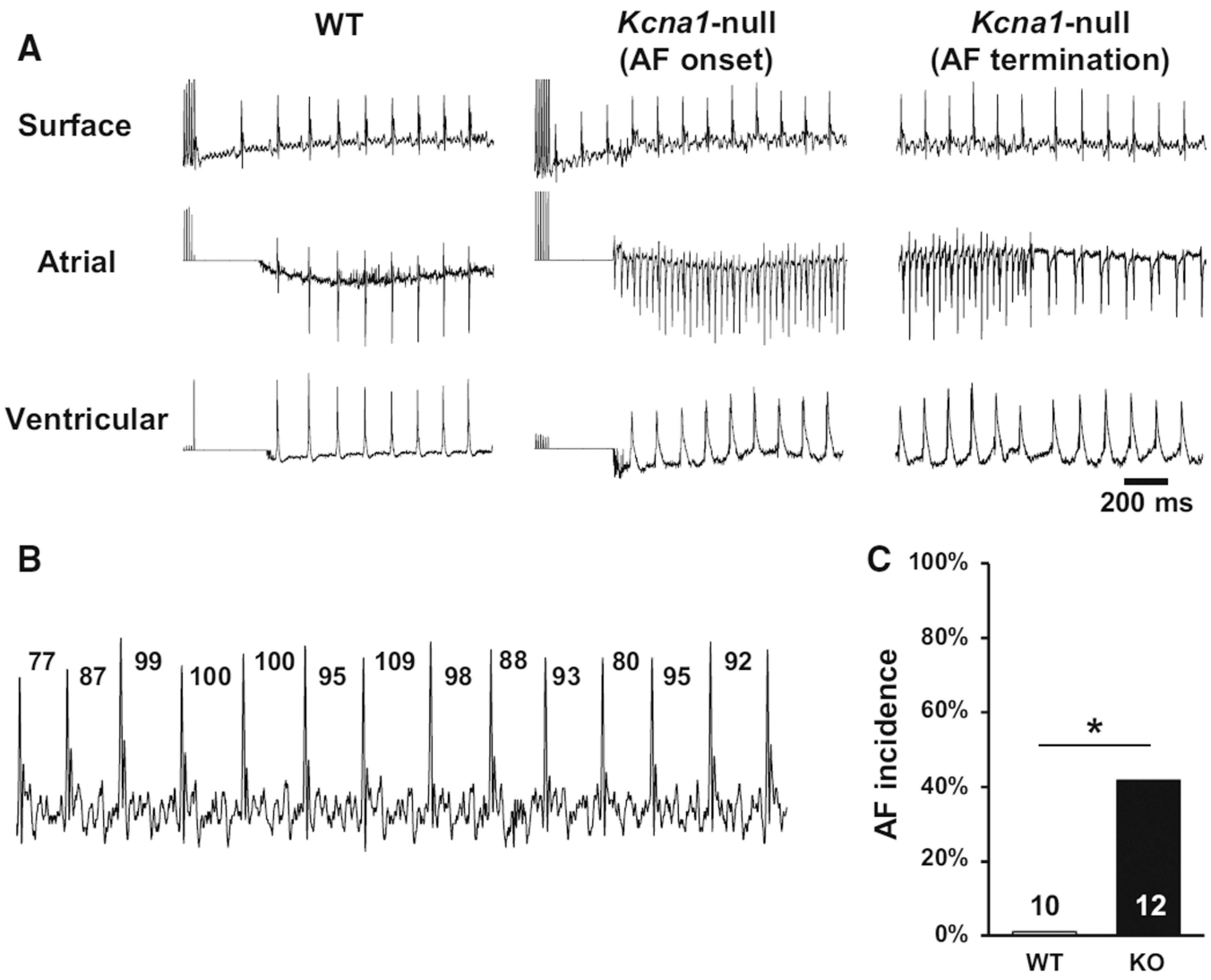

Fig. 1.

Mice lacking Kv1.1 channels are vulnerable to pacing-induced AF.

a Representative simultaneous recordings of surface ECG (lead I) and intracardiac atrial and ventricular electrograms after burst pacing in wild type (WT) and *Kcna1*-null (KO) mice. In the KO animal shown, pacing produced AF (*AF onset*) that lasted about 13 s before returning to normal sinus rhythm (*AF termination*). **b** During inducible AF in KO animals, the surface ECG exhibited absent P waves and irregular RR intervals, which are shown labeled in milliseconds. **c** KO mice showed significantly higher incidence of pacing-induced AF than WT controls. $*P < 0.05$

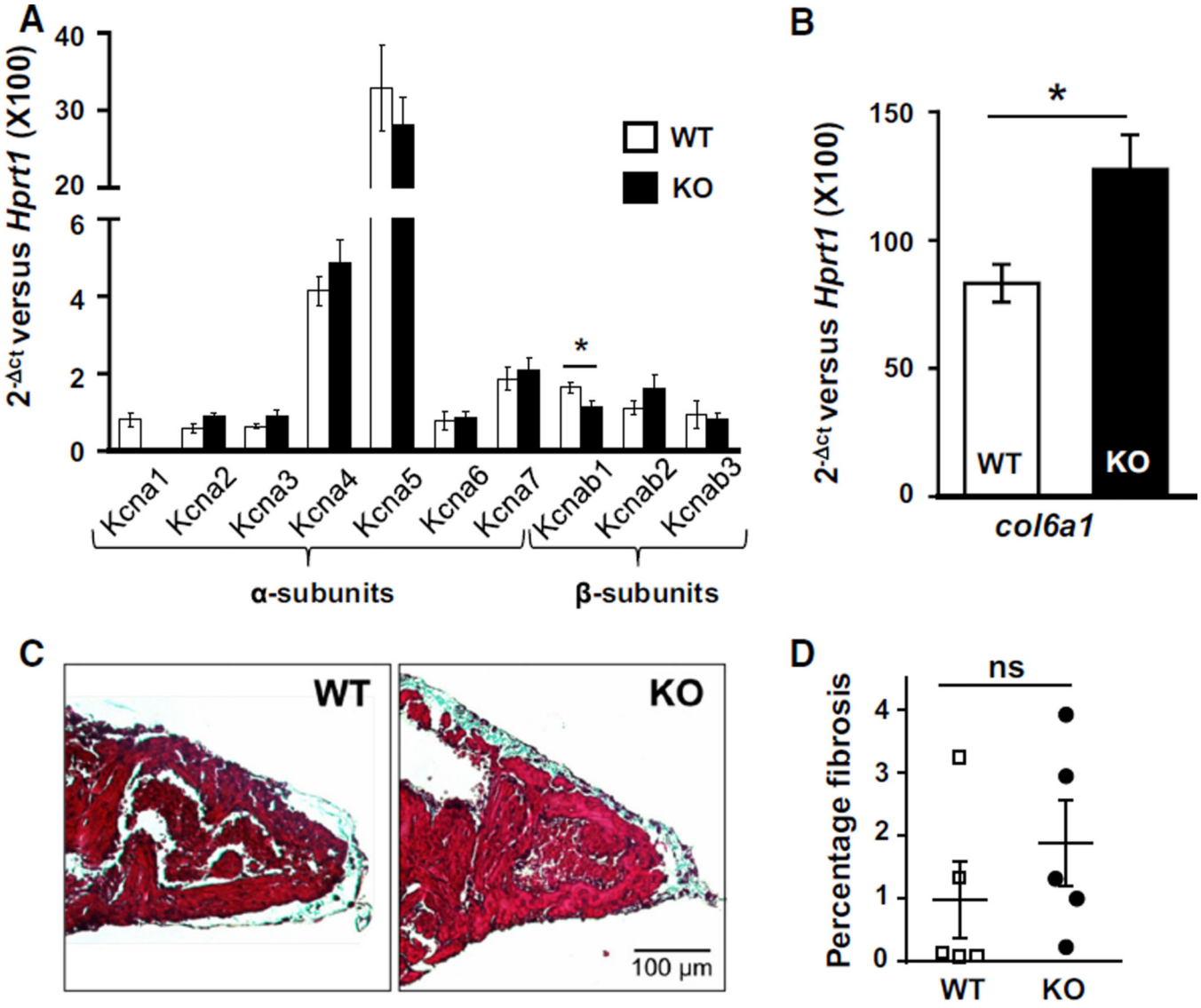

Fig. 2.

Kcna1-null mice exhibit minimal Kv1.x channel remodeling and atrial fibrosis. **a** Real-time PCR expression analysis of Kv1.x potassium channel α- and β-subunit genes in atria from KO and control WT mice ($n = 5$ mice per genotype). **b** Real-time PCR analysis of *col6a1* mRNA levels ($n = 5$ mice per genotype). **c** Representative samples of atria from WT and KO animals stained with Masson's trichrome to visualize fibrosis which appears bluish. Images were chosen out of sections from 5 WT mice and 5 KO mice. **d** Quantification of the percentage of atrial fibrosis between genotypes. $^*P < 0.05$; *ns* not significant

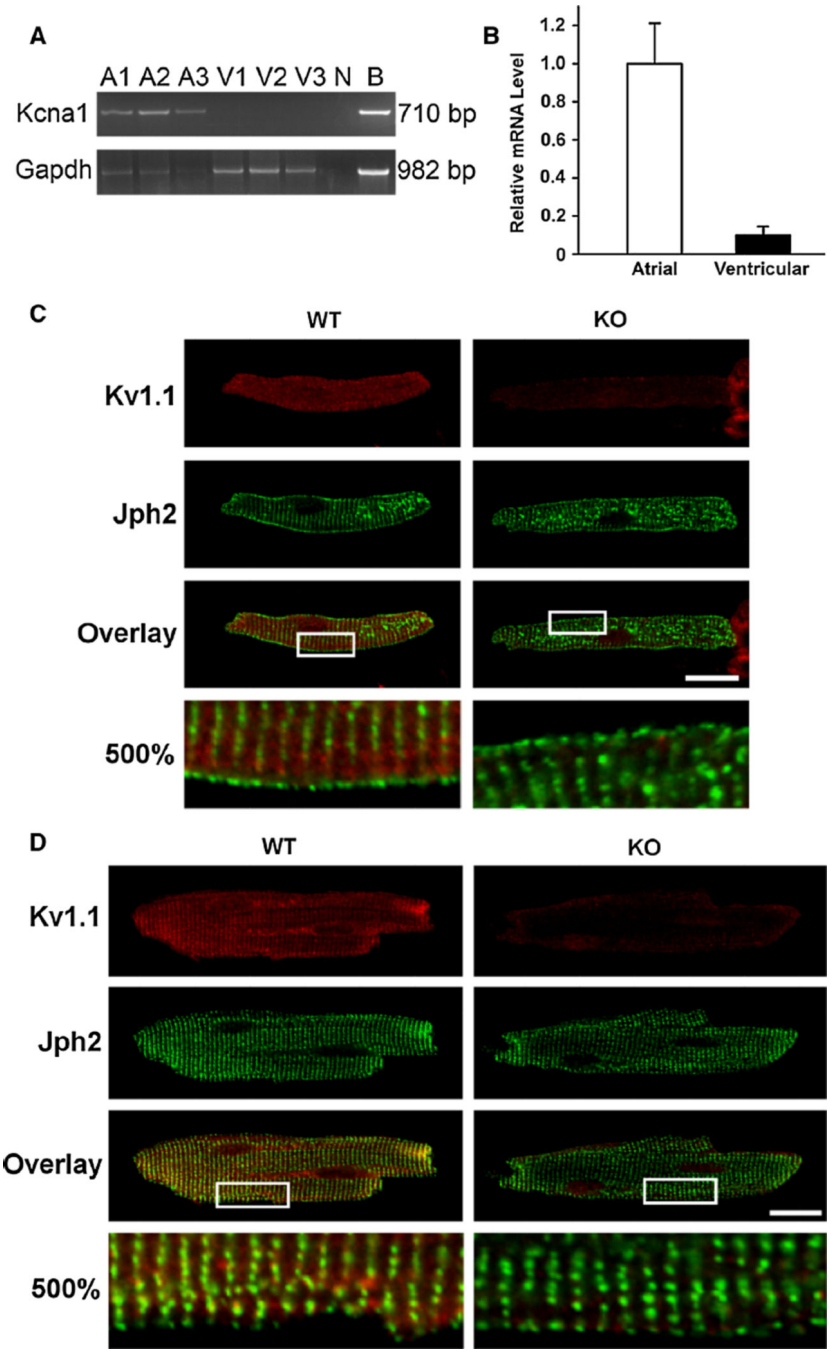

Fig. 3.

Kcna1 expression in mouse cardiomyocytes. **a** RT-PCR detection of *Kcna1* mRNA in isolated atrial (A) and ventricular (V) myocytes from three mice labeled 1–3. Brain tissue (B) was used as a positive control, while no cDNA (N) was used as a negative control. **b** Quantitative RT-PCR shows that *Kcna1* mRNA levels (normalized to *Rpl7*) are about tenfold more abundant in atrial myocytes than in ventricular (n = 3 mice; $P = 0.07$, paired t test). Immunostaining of isolated atrial (**c**) and ventricular (**d**) myocytes isolated from adult mice and co-stained with antibodies against Kv1.1 and Junctophilin-2 (Jph2), a t-tubule protein.

The gain was increased in the ventricular images relative to the atrial images to allow visualization of Kv1.1 immunoreactivity, which is much less intense in ventricular myocytes. The boxed regions in the overlay images are shown magnified 500 % in the bottom panels. Representative images were chosen out of 15 cells (7 atrial and 8 ventricular myocytes) from 2 WT mice and 8 cells (5 atrial and 3 ventricular myocytes) from 1 KO mouse. *Scale bars* 20 μm

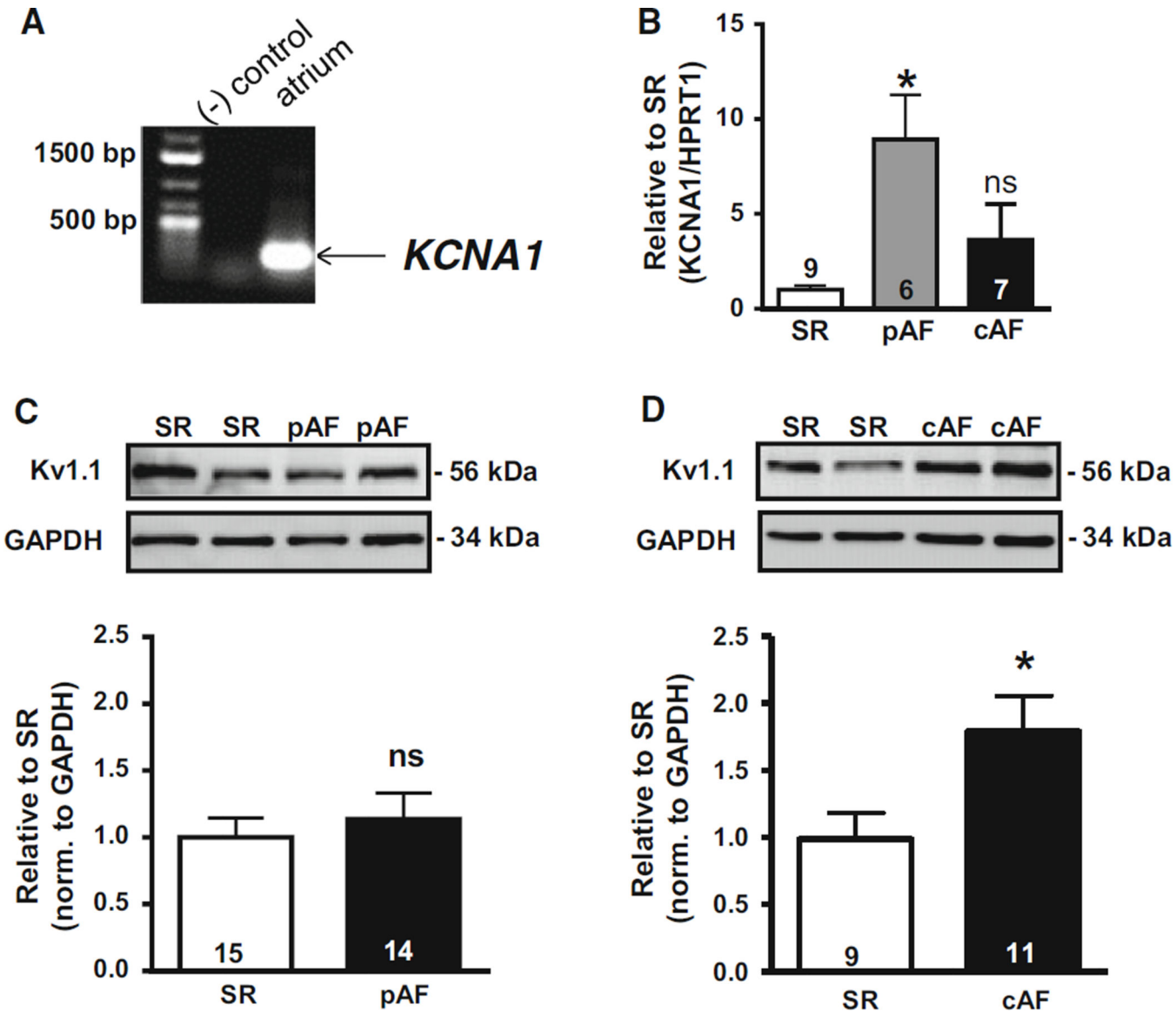

Fig. 4.

KCNA1 mRNA and protein expression in human atria. **a** RT-PCR detection of *KCNA1* mRNA in human atria. **b** mRNA levels (mean ± SEM) of *KCNA1* in patients with chronic AF (cAF) and paroxysmal AF (pAF) relative to sinus rhythm (SR). Representative Western blots of Kv1.1 protein with corresponding densitometric quantification (mean ± SEM) of protein levels in patients with pAF (**c**) and cAF (**d**) relative to SR. **P* < 0.05 vs. SR; *ns* not significant. *Numbers* in *bars* indicate atrial samples

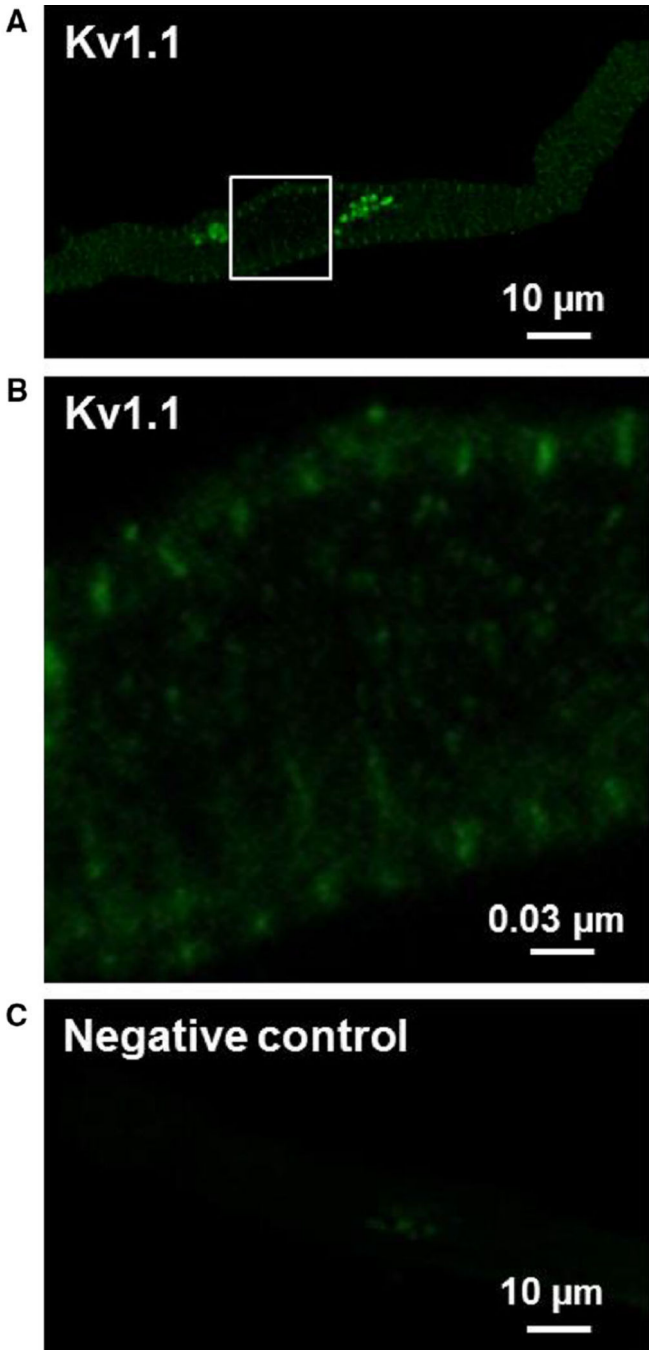

Fig. 5.

Kv1.1 immunoreactivity in isolated human atrial cardiomyocytes. Representative confocal images of Kv1.1-positive immunostaining (**a**, **b**) and a negative control (**c**). Kv1.1 immunoreactivity showed a strong fluorescent signal throughout the cell and a tight striated pattern which overlapped with the Z-line. In negative controls, primary antibody was omitted and cells were labeled only with the secondary antibody revealing an absence of nonspecific, background staining

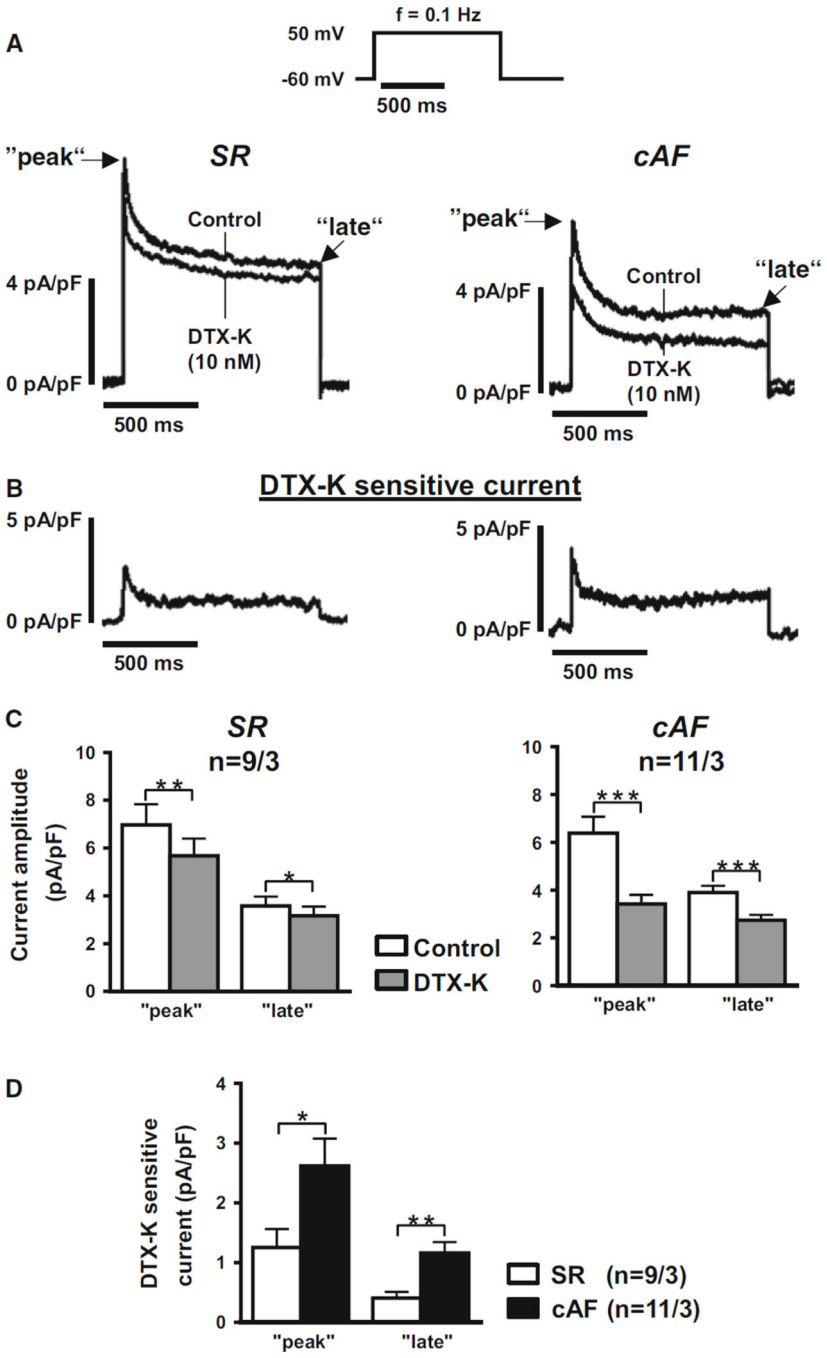

Fig. 6.

Dendrotoxin-K sensitive outward current in isolated human atrial myocytes. **a** Averaged current traces recorded from human atrial myocytes from patients in sinus rhythm (SR) or chronic AF (cAF). Current traces show control measurements at baseline followed by application of 10 nmol/L dendrotoxin-K (DTX-K) to specifically block Kv1.1 channels. The voltage step protocol used for recordings is shown at the *top*. **b** Traces show the averaged current difference representing the dendrotoxin-K sensitive component. **c** Amplitudes of the peak and late phases of the outward K^+ currents (mean ± SEM) before (control) and after

application of DTX-K in atrial myocytes from SR and cAF patients. **d** Amplitudes of the peak and late phases of the DTX-K sensitive current difference (mean ± SEM) in atrial myocytes from SR and cAF patients. *$P < 0.05$, **$P < 0.01$, ***$P < 0.001$ vs. corresponding means under control conditions using Student's paired (**c**) and unpaired (**d**) t test, respectively. The n values indicate myocyte/patient numbers.

Table 1

Patient characteristics

	SR	PAF	CAF
Patients, *n*	32	14	23
Gender, m/f	24/8	10/4	15/8
Age, years	64.09 ± 11.2	66.9 ± 10.1	67.78 ± 9.41
Body mass index, kg/m^2	28.09 ± 5.79	29.54 ± 7.53	29.23 ± 4.21
CAD, *n* (%)	17 (53)	4 (29)	8 (35)
AVD, *n* (%)	8 (25)	6 (43)	6 (26)
MVD, *n* (%)	0 (0)	1 (7)	5 (22)
CAD + AVD, *n* (%)	7 (22)	4 (29)	5 (22)
Hypertension, *n* (%)	28 (88)	14 (100)	22 (96)
Diabetes, *n* (%)	7 (22)	4 (29)	8 (35)
Hyperlipidemia, *n* (%)	29 (91)	12 (86)	17 (74)
LVEF			
Normal, *n* (%)	16 (50)	6 (43)	11 (48)
Mildly reduced, *n* (%)	10 (31)	2 (14)	3 (13)
Moderately reduced, *n* (%)	4 (13)	4 (29)	6 (26)
Severely reduced, *n* (%)	1 (3)	2 (14)	3 (13)
β-Blockers, *n* (%)	20 (62)	14 (100)	19 (83)
Digitalis, *n* (%)	2 (6)	2 (14)	7 (30)
Amiodarone, *n* (%)#	0 (0)	0 (0)	1 (7)
Other AADs, *n* (%)	0 (0)	0 (0)	0 (0)
ACE inhibitors, *n* (%)	19 (59)	8 (57)	12 (52)
AT1 blockers, *n* (%)	6 (19)	2 (14)	3 (13)
Dihydropyridines, *n* (%)	8 (25)	4 (29)	3 (13)
Diuretics, *n* (%)	9 (28)	10 (71)	11 (48)
Nitrates, *n* (%)	1 (3)	2 (14)	3 (13)
Lipid-lowering drugs, *n* (%)	22 (69)	11 (79)	14 (61)
Biguanides, *n* (%)#	2 (7)	2 (18)	1 (7)
Sulfonylurea derivatives, *n* (%)#	1 (4)	0 (0)	0 (0)
Insulin, *n* (%)#	0 (0)	3 (27)	2 (14)
OAC, *n* (%)#	0 (0)	5 (45) **	13 (93) ***
Antiplatelet drugs, *n* (%)#	23 (88)	8 (73)	6 (43) *

AAD antiarrhythmic drug, *ACE* angiotensin converting enzyme, *AT* angiotensin receptor, *AVD* aortic valve disease, *CAD* coronary artery disease, *CAF* chronic atrial fibrillation, *LVEF* left ventricular ejection fraction (normal, ≥55 %; mild impairment, 45–54 %; moderate impairment, 30–44 %; severe impairment,<30 %), *MVD* mitral valve disease, *OAC* oral anticoagulation, *PAF* paroxysmal atrial fibrillation, *SR* sinus rhythm

* $P < 0.05$,

** $P < 0.01$,

*** $P < 0.001$ versus SR from Fisher exact test followed by Bonferroni multiple comparisons procedure for categorical variables

[#]Data were not available for 6 SR, 3 pAF and 9 cAF patients

Table 2

Baseline ECG parameters in WT and *Kcna1*-null mice

	WT (*n* = 10)	KO (*n* = 12)	*P*
Age, months	4.0 ± 0.3	4.1 ± 0.3	0.68
Heart mass, g[a]	160 ± 11	173 ± 12	0.48
Heart:body ratio, mg/g[a]	4.8 ± 0.2	5.3 ± 0.3	0.23
PQ, ms	27.0 ± 0.6	27.0 ± 1.2	1.00
QRS, ms	7.8 ± 0.4	6.9 ± 0.2	0.04
QT, ms	34.0 ± 1.6	34.8 ± 1.3	0.69
QTc, ms	57.2 ± 1.6	57.6 ± 1.7	0.88
RR, ms	96.8 ± 2.1	98.3 ± 2.6	0.67
SCL, ms	96.7 ± 2.0	98.3 ± 2.5	0.65
AV, ms	33.4 ± 0.9	33.8 ± 0.9	0.73
SNRT, ms	122.0 ± 6.2	125.5 ± 8.4	0.75
RA ERP, ms	28.7 ± 2.0	31.7 ± 2.1	0.34
AV ERP, ms	40.1 ± 1.9	41.5 ± 3.2	0.75

Data are expressed as mean ± SEM. Student's *t* test used to compare intragroup differences. *P* values between WT and KO mice are shown *SCL* sinus cycle length, *AV* atria-to-ventricle conduction time, *SNRT* sinus node recovery time, *RA ERP* right atrial effective refractory period, *AV ERP* atrioventricular node effective refractory period

[a]Data derived from 9 KO and 6 WT animals